Removal of Basic Blue 3 from the Aqueous Solution with Ternary Polymer Nanocomposite: Swelling, Kinetics, Isotherms and Error Function

[1]Selcan Karakuş, [2]Sedef Şişmanoğlu, [1]Gizem Akdut, [1]Öykü Ürk, [1]Ezgi Tan
[1]Tuba Şişmanoğlu* and [1]Ayben Kilislioğlu
[1]Istanbul University, Engineering Faculty, Department Chemistry, 34320 İstanbul,TURKEY,
[2]Karabuk University, Engineering Faculty, Metallurgy and Materials Engineering, Karabuk,TURKEY.
tusase3@gmail.com*

(Received on 17th December 2015, accepted in revised form 29th August 2016)

Summary: Ternary nanocomposite (Gum Arabic / PVA / Alginate) adsorbent was prepared by a cost effective method for dyes removal, because gum arabic and alginate are the cheapest materials. Gum arabic is a natural gum. Alginate that has long carboxylate functional group is a biosorbent. In this study, Gum arabic/PVA/Alginate was prepared that this absorbent has the high specific surface area. BET was measured as 12.93 m^2/g. Swelling of adsorbent was determined at different pH. For the maximum swelling ratio was obtained at pH 6.88≅7, adsorption experiments were studied by the batch method. Freundlich, BET and Langmuir isotherm methods were applied at different concentrations and constant temperature 25° C. Finally, the adsorption capacity of the nanocomposite was calculated as 200 mgg^{-1}. The different adsorption kinetic models were studied at temperature from 25°C to 45°C and different concentrations. The thermodynamic parameters as ΔH^o, ΔG^o, and ΔS^o were calculated.

Keywords: Cationic dyes, Adsorption, Ternary polymer nanocomposite, Isotherms, Kinetics

Abbreviations: BB3, Basic blue 3; GPVAA, Gum Arabic / PVA / Alginate

Introduction

Water pollution is one of the environment problems which will cause severe impact to living organisms. Some of these dyes are toxic and carcinogenic, such as azo, anionic (acidic), cationic (basic) dyes. Therefore, the necessity of dye wastewater undergo pretreatment prior of disposal is important. Basic dyes (cationic) are a commercial available synthetic dyes and these dyes are widely used at textile industry. Basic dyes are used in textile such as silk, leather, paper, cotton, ink and copying paper in office supplies industry. Basic Blue 3 BB3 is an oxazine cationic dyes which create positively charged ions.

Gum arabic, also known as acacia gum, is a natural gum made of hardened sap taken from two species of the acacia tree. It is cheap and natural polymer. Gum arabic is used primarily in the food industry as a stabilizer. Both Gum Arabic and Alginate are content polysaccharides and glycoproteins groups. Polysaccharides and glycoproteins have alcohol and carboxyl groups. When extra carboxyl groups are formed by matching these groups, the cationic dyes having cationic groups are easily adsorbed. So, Gum Arabic / PVA / Alginate (GPVAA) was preferred for adsorption of Basic Blue 3 (BB3).

Nanocomposites consist with nano-size distribution of multiple materials. Especially, several binary studies of polymer-clay have been made for nanomaterial. Using crosslinkers, the polymer / clay or polymer / polymer mixtures are obtained nanomaterials [1]. As adsorbent, alg [2], agricultural waste [3-5], clay [6, 7], resin [8], polymer [9], carbon nanotubes (CNT) [10], nanocomposites [11] is used for removal of dangerous waste such as dyes, pesticide and heavy metal. In the recent years remarkable amount of researches have been done adsorption of BB3 on the low cost and easily available alternative adsorbents, such as Quartenised Sugar Cane Bagasse [12], *Corynebacterium glutamicum* biomass [13], Aleppo pine-tree sawdust [14] sepiolite, fly ash and apricot shell activated carbon [15], Lewatit MonoPlus SP 112 (SP 112), functionalized Dowex Optipore SD 2 (SD 2) and non-functionalized Amberlite XAD 1180 (XAD 1180) [16] etc. Although these researchers use the cheapest adsorbent,adsorption capacity of these adsorbents are very low [12-15] .Whereas, cost of adsorbents with high adsorption capacity is very high [16].

Therefore, the aim of this study was to investigate the capability of ternary nanocomposite to remove basic dye, Basic Blue 3 (BB3). In this study, before the swelling behaviour of the ternary

*To whom all correspondence should be addressed.

nanocomposite (Gum Arabic /PVA/Alginate) was characterized by gravimetrically for the different pH medium and then the adsorption of BB3 was studied on this ternary nanocomposite. The adsorption of BB3 onto Gum Arabic /PVA/Alginate from aqueous solutions was determined by UV-vis spectroscopy. The adsorption isotherms models of BB3 were studied at 25 ^{o}C and different concentrations for Langmuir, Freundlich and BET. The adsorption kinetic studies of BB3 were investigated at temperature between 25 °C and 45 °C and different concentrations.

Experimental

Chemicals

Polyvinyl alcohol (PVA) (average molecular weight: 30.000-70.000, 85% hydrolyzed), and sodiumalginate (Alginic acid sodium salt from brown algae, viscosity ≥ 2.000 cP, 2 % (25 °C) were purchased from Sigma-Aldrich. Glutaraldehyde (50% solution in water) was purchased from Merck. The textile dye Basic Blue 3 (BB3) were purchased from Aykar Boya (Turkey).

Instrumentation

For the spectrophotometric measurements were used CHEMBIOS Optimum-One UV-visible spectrophotometer. The maximum absorbance value of BB3 was measured at 669 nm. Structure of the ternary adsorbent was determined by FTIR (Perkin Elmer Precisely Spectrum One FTIR) before adsorption and after adsorption. Determination of wet / dry weight values of this ternary adsorbent were made by analytical balance (RADWAG AS 220 / C / 2).

Preparation of Gum Arabic / PVA / Alginate Ternary Nanocomposite (GPVAA)

0.1 g of PVA was solved in 10ml deionized water at 50^{o}C and 0.1 g of Gum Arabic were added into the solution and the mixture was stirred for 2 h. After 0.01 g of sodiumalginate and cross-linker (glutaraldehyde) were added to this mixture. The ternary nanocomposites films were dried at 45 ^{o}C for 12 h.

Procedure

Batch adsorption experiments were carried out by using GPVAA as the adsorbent. Stock solution of BB3 (500 ppm) was prepared in the distilled water. Before, the adsorbate concentration were adjusted between 295 ppm and 40 ppm, then absorbance values of these samples were measured by UV-vis spectrophotometre at 669 nm. The calibration graph of absorbance versus concentration followed a linear Lambert–Beer relationship [17].

Adsorbate (BB3) volume 10 ml and adsorbent (GPVAA) amount 0.04 g were taken in the adsorption experiments. So, the V/m ratio value was fixed as 0.25 L g^{-1} and pH of solutions were measured as 6.88 during adsorption process. Kinetic experiments of adsorption were studied at the different temperatures (25-45 ^{o}C) and the kinetic study was fixed at time intervals, as 5, 10, 30, 45, 75, 100 minutes. All samples were centrifuged for 10 minutes at constant string speed of 4000 rpm. Adsorption isotherms of BB3 were performed between 40 and 295 ppm concentrations at 25 ^{o}C temperature. Before and after adsorption of basic blue 3 (BB3) onto GPVAA are as seen in Fig. 1. Amount of adsorbed (mg g^{-1}) was calculated by using the following relationships [18]. For five concentrations, the different adsorption kinetic models were studied at temperature from 25 °C to 45 °C. For each temperature, equilibrium of adsorption BB3 on GPVAA has been reached at 100 minutes as shown in Fig. 2. Also, the gravimetric procedure was used to calculate the equilibrium swelling ratio of the GPVAA samples in water and in buffer solution of pH 4-11 at 25 °C. For all samples, the surface of sample was dried using filter paper and weighed.

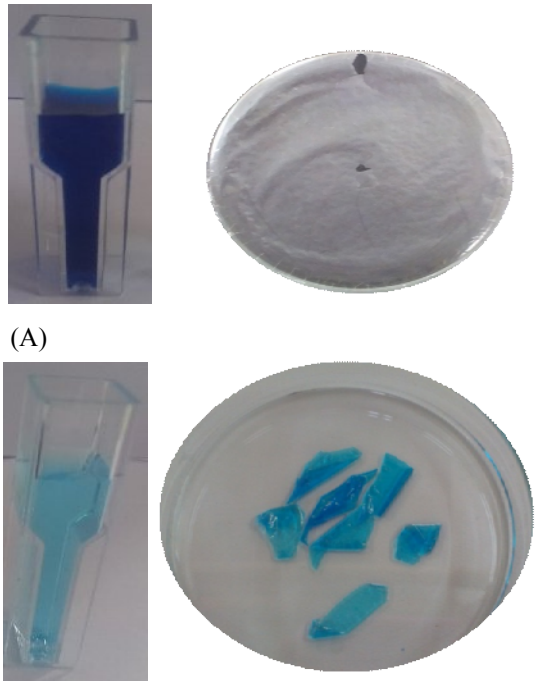

(A)

(B)

Fig. 1: For 295 ppm concentration of BB3 on GPVAA (A) before adsorption, (B) after adsorption

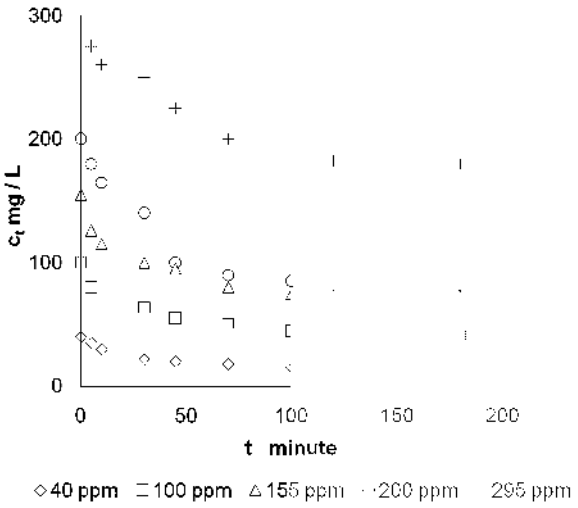

Fig. 2: Plots of concentrations of BB3 vs time at 25°C.

Results and Discussion

Swelling rations of GPVAA

The equilibrium swelling ratio of the GPVAA samples were determined in water and in buffer solution of pH 4-11 at 25 °C. The equilibrium swelling ratio is defined as follows equation 1:

$$\%\text{Swelling ratio} = \frac{W_s - W_d}{W_d} \times 100 \quad (1)$$

where; w_s the weight of the swollen sample, w_d the weight of the dried sample.

Maximum swelling ratio to reach the equilibrium states was occurred in water for 45 minute % 701 at pH 4. But, this maximum swelling ratio was obtained for 180 minute % 712.35 at pH 7, as shown in Table-1. For pH 4, GPVAA was disintegrated after 45 minutes. But this absorbent (GPVAA) was cleaved after 15 minutes at pH 11 [19, 20].

Table-1: % Swelling ratio of GPVAA in the different pH.

Time (min.)	pH 4	pH 7	pH 11
0	0.00	0.00	0.00
15	170.61	80.99	388.27
30	415.45	101.60	-
45	701.01	232.27	-
60	-	428.98	-
120	-	601.01	-
180	-	712.35	-

Characterization

The BET surface areas of Gum arabic/PVA/Alginate are measured. Before adsorption, the pore diameters of this adsorbate and the surface areas have found as respectively 12.93 m^2g^{-1} and 36.5 nm. After adsorption, the pore diameters of this adsorbate and the surface areas have found as respectively 5.68 m^2g^{-1} and 39.85 nm

For FTIR spectra of BB3, the peaks observed aromatic rings, CH_3 bond bending and C=N bond stretching, respectively at the 2970-2870 cm^{-1}, 1590 cm^{-1}. The structure of dye molecule have aryl C-N and alkyl C-N stretching bands and thes bands are monitored a peak respectively at 1340-1267 cm^{-1} and 1150-1000 cm^{-1}.

For FTIR spectra of GPVAA, 3400 cm^{-1} indicates the possible of -OH on the surface. 2940 and 1325 cm^{-1} show that the peaks are C-H bond bending. Also, 1750 cm^{-1} region can be assigned to the C=O stretching and N-H bond bending at 1540 cm^{-1}. The peaks located at the 1150-1000 cm^{-1} wave numbers belong to C-O vibrations in the rings.

For FTIR of BB3 + GPVAA, BB3 belonging to, the peaks disappeared between 1590 and 1000 cm^{-1} wavenumbers. Also, GPVAA belonging to, the peaks of C-O bond bending deformed at the 1150-1000 cm^{-1} as seen in Fig. 3.

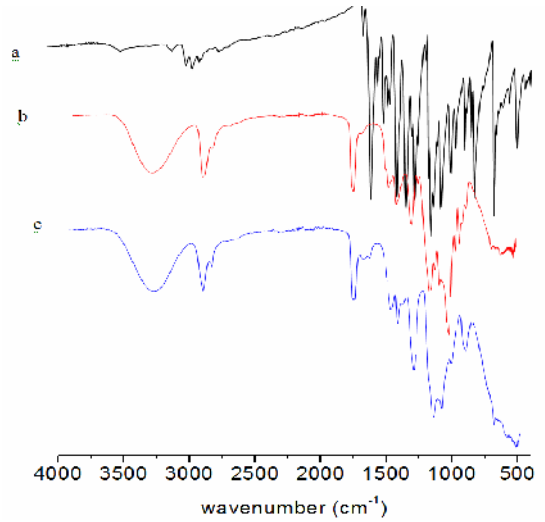

Fig. 3: FTIR curves; (A) BB3, (B) GPVAA, (C) BB3+ GPVAA.

SEM micrographs of GVPAA before adsorption, the cracks and slits were observed on rough surface of GPA. After adsorption of BB3, these cracks and slits were completely disappeared as seen in Fig. 4. The surface of ternary nanocomposite was smooth. In this case suggest that adsorption process occurred onto adsorbent surface.

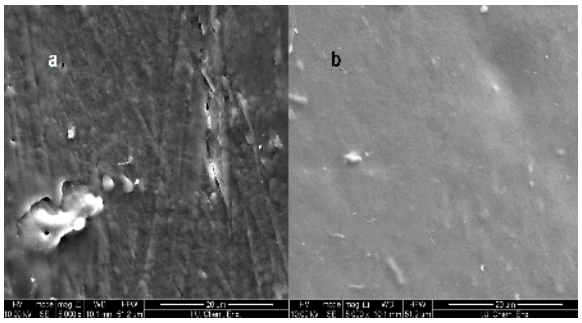

Fig. 4: SEM micrographs of GPVAA; (a) in the absence of adsorbate molecules (b) after BB3 adsorption.

Kinetics and Thermodynamic

For kinetics mechanism of adsorption processes, the pseudo-first-order, pseudo-second order and intra-particle diffusion equations were applied to model the kinetic of BB3 adsorption on GPVAA at three temperatures. For the calculation of kinetics, each concentration of BB3 equilibrium time of adsorption was taken as 100 minutes.

The adsorption process in a given system were determined in this study using the pseudo-first-order rate equation as estimated by [21,22] and the pseudo-second-order equation [23] and the intra-particle diffusion [24]. For each concentrations of BB3, the rate of constants of pseudo-first order has changed with increasing temperature as unsteady. The rate of constants of intra-particle diffusion has changed with increasing temperature for the lowest concentrations of BB3 as irregularly. But, these rate of constants have increased with increasing temperatures for the highest concentrations of BB3 as regularly. For the intra-particle diffusion ,the rate controlling step of adsorption process was realized by using Weber and Morris model, as seen in Table-2 and 3. Also, q_t versus $t^{1/2}$ are shown in Fig.5. For this adsorption mechanism, the intra-particle diffusion has occurred in single step for each concentration and these graphics have not gone through the point of origin. This means that the solute molecules is spread by diffusion to the boundary layer and the adsorption mechanism can thought to be very complex [25].

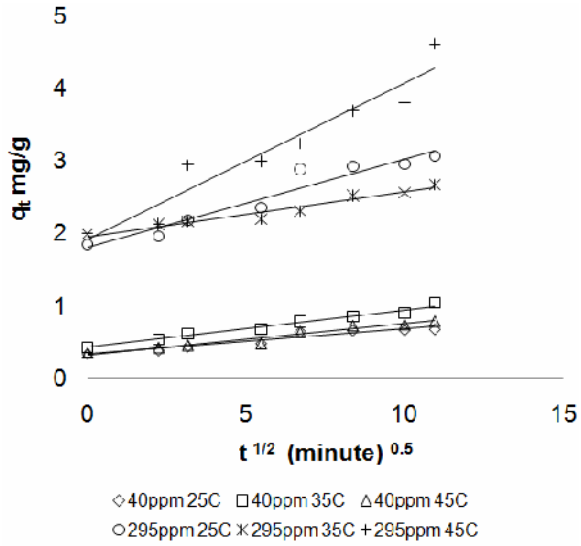

Fig. 5: Weber and Morris model for adsorption of BB3 on GPVAA.

Table-2: Kinetic parameters for 40, 100, 155 ppm.

40 ppm									
$q_{experimental}$ (mgg^{-1})	t/°C	k_1 (min^{-1})	$q_{calculated}$ (mgg^{-1})	R^2	k_2 ($gmg^{-1}min^{-1}$)	$q_{calculated}$ (mgg^{-1})	R^2	k_i ($mgg^{-1}t^{-0.5}$)	R^2
10.2	25	0.012	2.40	99	0.051	11.0	98	0.051	99
12.1	35	0.021	2.20	95	0.062	12.0	98	0.042	94
14.2	45	0.031	1.88	95	0.086	14.8	99	0.034	90

100 ppm									
$q_{experimental}$ (mgg^{-1})	t/°C	k_1 (min^{-1})	$q_{calculated}$ (mgg^{-1})	R^2	k_2 ($gmg^{-1}min^{-1}$)	$q_{calculated}$ (mgg^{-1})	R^2	k_i ($mgg^{-1}t^{-0.5}$)	R^2
12.8	25	0.031	5.56	96	0.011	13.2	97	0.094	94
18.2	35	0.019	3.20	92	0.040	19.0	98	0.060	96
19.4	45	0.022	2.16	98	0.062	19.6	99	0.045	91

155 ppm									
$q_{experimental}$ (mgg^{-1})	t/°C	k_1 (min^{-1})	$q_{calculated}$ (mgg^{-1})	R^2	k_2 ($gmg^{-1}min^{-1}$)	$q_{calculated}$ (mgg^{-1})	R^2	k_i ($mgg^{-1}t^{-0.5}$)	R^2
28.9	25	0.018	6.68	98	0.020	29.8	100	0.152	93
35.1	35	0.007	3.44	93	0.034	36.1	97	0.067	97
41.0	45	0.018	1.88	99	0.130	42.3	100	0.040	96

Table-3: Kinetic parameters for 200 and 295 ppm.

200 ppm									
$q_{experimental}$ (mgg^{-1})	t/°C	k_1 (min^{-1})	$q_{calculated}$ (mgg^{-1})	R^2	k_2 ($gmg^{-1}min^{-1}$)	$q_{calculated}$ (mgg^{-1})	R^2	k_i ($mgg^{-1}t^{-0.5}$)	R^2
75	25	0.015	3.12	93	0.057	75.68	100	0.061	95
50.5	35	0.023	5.92	94	0.034	50.8	100	0.121	93
43.4	45	0.010	10.0	97	0.011	43.6	97	0.220	98

295 ppm									
$q_{experimental}$ (mgg^{-1})	t/°C	k_1 (min^{-1})	$q_{calculated}$ (mgg^{-1})	R^2	k_2 ($gmg^{-1}min^{-1}$)	$q_{calculated}$ (mgg^{-1})	R^2	k_i ($mgg^{-1}t^{-0.5}$)	R^2
164	25	0.010	0.80	66	0.28	165	100	0.021	64
163	35	0.021	1.64	94	0.17	163	100	0.034	91
162	45	0.011	2.20	88	0.11	161	100	0.053	90

The best-fit was found on the pseudo-second-order model. The rate constant of pseudo-second-order increased with increasing temperature for 40-155 ppm and decreased with increasing temperature for 200 and 295 ppm, as seen in Table 2-3. For k_2 values, it was observed that both the calculation ($q_{e,cal}$) and experimental ($q_{e,exp.}$) findings were compatible with each other.

Thermodynamic parameters was calculated using the Arrhenius as defined [26] and the Eyring equations [27] .

The free energy of change ΔG^o was obtained from equation 2:

$$\Delta G^o = \Delta H^o - T\Delta S^o \qquad (2)$$

The adsorption mechanism was physical adsorption, because of the value of E_a between 40-100 kJ mol^{-1} as seen in Table-4. As seen in Fig. 6, the positive values activation energy of BB3 were calculated for 40, 100, 155 ppm, but the negative values activation energy of BB3 were found for 200 and 295 ppm. The negative activation energy suggest that the reactions are a barrier less, because of diffusion of water molecules into adsorbent (GPVAA) [28].

Table-4: According to the rate constant of pseudo-second-order model thermodynamic parameters.

Con /ppm	ΔE_a $kjmol^{-1}$ (25°C-45°C)	ΔH^o $kjmol^{-1}$ (25°C-45°C)	ΔG^o $kjmol^{-1}$ (25°C)	ΔS^o $jmol^{-1}K^{-1}$ (25°C-45°C)
40	21.3	19	80.5	-207
100	68.5	66	83.9	-60.0
155	73.4	71	83.0	-40.8
200	-64.5	-67	80.0	-493
295	-40.5	-43	76.1	-400

The positive enthalpy change (between 40 and 155 ppm) indicates that the adsorption reaction is endothermic and the negative enthalpy change (between 200 and 295 ppm) suggests that the adsorption reaction is exothermic, as seen in Table-4. In this study, the interaction between BB3 and the adsorbent was calculated as the negative of the entropy change ΔS^o. The negative value of ΔS^o suggests that the adsorption process involves an associative mechanism. The adsorption leads to order through the formation of an activated complex between the adsorbate and adsorbent. These negative values indicate that the transition from disorder to order and the adsorption process is made possible. The values of ΔG^o are positive at all temperatures suggesting that adsorption reactions require some energy from an external source to convert reactants into products. As a result, this adsorption reaction is nonspontaneous.

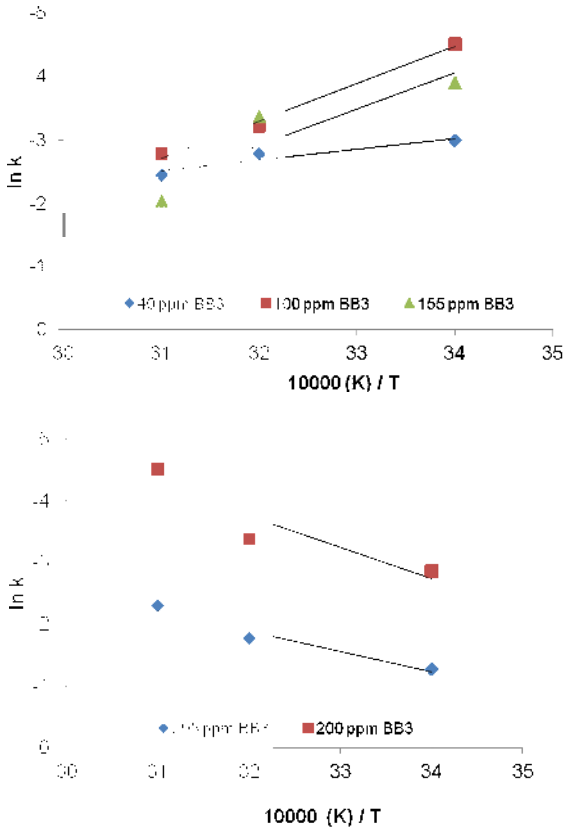

Fig. 6: Plot of ln k vs 1/T fort he adsorption BB3 on GPVAA.

Adsorption isotherms

According to the swelling values % vs time, the best of study condition for adsorption of BB3 was obtained pH 7. Therefore, all of adsorption isotherm experiments were studied at pH 6.88≅7 and the constant temperature (25 °C). The shape of isotherms was obtained for BB3 on the adsorbent L-type, as shown in Fig. 7a. While adsorption data until 100 minutes were using for kinetic experimental, relevant data of adsorption isotherm (BB3- GPVAA) were accepted up to 180 minutes, as shown in Fig. 2. When GPVAA is compared with other adsorbants, its adsorption capacity is very high. Also, equilibrium time of adsorption BB3 on GPVAA is faster than other adsorption studies of BB3 [29- 31].

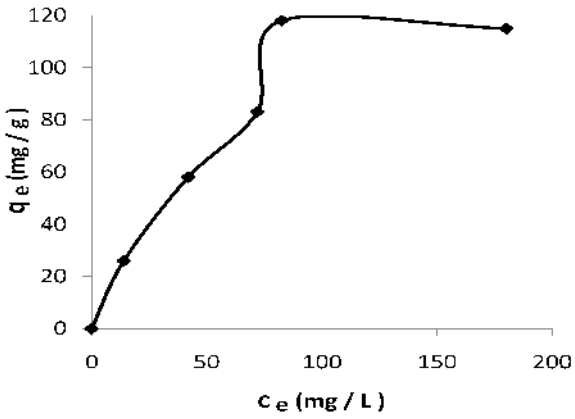

(A)

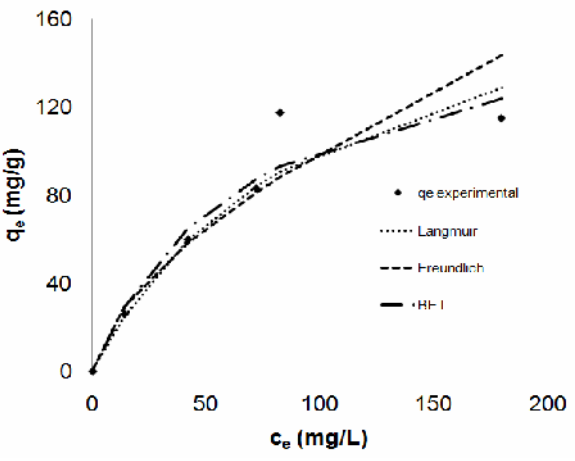

(B)

Fig. 7: (a) Adsorption isotherms of BB3 on GPVAA b) Comparison of experimental data with theoretical isotherm curves for BB3 adsorption on the GPVAA at 25°C temperature.

The adsorption isotherm for the BB3 adsorbed on the GPVAA adsorbent was fitted to the Langmuir ,Freundlich, BET isotherms. The linearized equation of Langmuir model is as shown by equation 3.

$$\frac{1}{q_e} = \frac{1}{q_m\, b\, c_e} + \frac{1}{q_m} \qquad (3)$$

where, q_e the amounts of dye adsorbed on adsorbent at equlibrium (mg g^{-1}), c_e the equilibrium concentration of adsorbate (mg L^{-1}), q_m the Langmuir constants related to the maximum adsorption capacity (mg g^{-1}), b the Langmuir constants related to the energy of adsorption (L mg^{-1}).

The Freundlich equationis usually fitted to the logarithmic form of the equation 4,

$$\log x_e = \log K_F + n \log c_e \qquad (4)$$

where, x_e amount adsorbed (mg g^{-1}), K_F Freundlich constant related to adsorption capacity, n Freundlich constant related to adsorption intensity.

Stephen Brunauer, Paul Emmet and Edward Teller (BET isotherm) is shown as equation 5

$$\frac{c_e}{x_e\,(c_o - c_e)} = \frac{1}{X_{max}\,k} + \frac{c_e\,(k-1)}{c_o\,X_{max}\,k} \qquad (5)$$

where, c_t the concentration of adsorbate at any time (mg L^{-1}), c_o the concentration of BB3 at saturated solution (for this study, 10000 mg L^{-1}), X_{max} for BET, the maximum adsorption capacity (mg g^{-1}), k for BET, a constant related with the heat of adsorption.

The results indicate that Langmuir and BET provides better fit for the experimental data of BB3 on GPVAA. This process shows that first monolayer adsorption and then multilayer adsorptionis, as seen in Fig. 7a. The value of the maximum adsorption capacity (q_m or X_{max}) is maximum (200 mg g^{-1}) for adsorbent at 25 °C as seen in Table-5. When the maximum adsorption capacity of GPVAA is compared other adsorbents, it is observed that GPVAA has best adsorption capacity [29- 31].

Table-5: Adsorption isotherm models at 25°C.

Langmuir			
	q_m (mg g^{-1})	**b (L mg^{-1})**	**R^2**
	200	**0.01**	**99.1**
Freundlich			
	n	**K_F**	**R^2**
	0.63	**5.60**	**91**
BET			
	X_{max} (mg g^{-1})	**R^2**	
	196	**98.5**	

Error functions

For defining the optimization procedure necessitates an error function [32-34]. The fit of the isotherm and kinetic to the experimental equilibrium data to be able to evaluate with these error functions. For the concentration range, four different error functions were examined by minimizing the respective these error function in this work. The studied error functions shown as seen in Table-6. Also, the correlation coefficient values of the equilibrium isotherm models have calculated. The correlation value of freundlich isotherm model has been quite found lower and the high value of the error functions for freundlich isotherm, as seen in Table-7. For Langmuir and BET isotherms, the comparison of error function has calculated as χ^2 <ARE<EABS<SSE. Fig. 7b shows the comparison of experimental data with theoretical isotherm curves for adsorption of BB3 on the gum arabic/PVA/alginate at 25°C temperature. These curves suggest that the Langmuir and BET isotherm models have the best performance for fitting with experimental data. The same calculation has repeated for the kinetic experimental data. The correlation value of pseudo-second order model has been quite found higher and the lower value of the error functions for pseudo-second order model, as seen in Table-8. Also, the values of Chi-square test error (CHI) has matched to assess the best error function for selecting the kinetic model as shown in Table-8.

Table-6: Error Functions.

Error Analysis	Formula ($q_{e\ meas}$: Measured adsorption capacity; $q_{e\ calc}$: calculated adsorption capacity with models; n: the number of experimental data points)	Reference
The sum of the squares of the errors (SSE)	$\sum_{i=1}^{p}(q_{e,calc}-q_{e,meas})_i^2$	(32)
The sum of the absolute errors (EABS)	$\sum_{i=1}^{p}\lvert q_{e,calc}-q_{e,meas}\rvert_i$	(33)
The average relative error (ARE)	$\frac{100}{n}\sum_{i=1}^{p}\left\lvert\frac{q_{e,calc}-q_{e,meas}}{q_{e,meas}}\right\rvert_i$	(34)
Chi-square test error (χ^2)	$\sum_{i=1}^{p}\frac{(q_{e,calc}-q_{e,meas})_i^2}{q_{e,meas}}$	(14)

Table-7: For q_e (mgg^{-1}), the values of four different error functions of isotherm models of BB3 on Gum arabic/PVA/Alginate

Isotherms	SSE	EABS	ARE	CHI (χ^2)
Langmuir	729.4	43.7	8.5	8.0
Freundlich	1692.1	65.3	13.6	16.0
BET	921.3	45.2	10.6	9.7

Table-8: For q_e (mgg^{-1}), error functions of kinetic models between 40 and 295 ppm

Error models	SSE		EABS		ARE		CHI (χ^2)	
t/°C	pseudo-first order	pseudo-second order	pseudo-first order	pseudo-second order	pseudo-first order	pseudo-second order	pseudo-first order	pseudo-second order
25	32407.96	3.07	272.34	3.78	81.05	3.12	35057.49	0.11
35	29349.79	5.74	262.50	4.20	88.34	1.98	16618.20	0.09
45	28630.97	6.13	261.88	4.30	89.33	2.02	12751.21	0.09

Conclusions

1. Maximum swelling ratio of GPVAA was obtained for 180 minute % 712.35 at pH 7. Therefore, the removal of textile dye Basic Blue 3 (BB3) onto ternary nanocomposite GPVAA was investigated at pH 6.88≅7 and adsorption isotherm (BB3-GPVAA) was accepted up to 180 minutes.
2. The adsorption maximum capacity of this adsorbent is found 200 mg g^{-1} for concentration of BB3 between 40 and 295 ppm. Value of adsorption capacity of GPVAA in Freundlich isotherm is found 5.6.
3. This adsorption capacity is higher than studied other adsorbents. In addition, adsorption time of BB3 on ternary adsorbent (GPVAA) is quite short compared with the others adsorbent. As a result, ternary adsorbent (GPVAA) may best uptaken for basic blue 3 (BB3).
4. Analysis of kinetics data implied that pseudo-second order kinetics model provided a beter correlation of the experimantal results than pseudo-first order and intra-particle diffusion order.
5. Values of pseudo-second order kinetics model have obtained a better correlation of the experimental results than pseudo-first order and intra-particle diffusion order.
6. The negative value of ΔS^o indicate that the passage from disorder to order and the adsorption process is made possible. The values positive of ΔG^o suggest that adsorption reactions require some energy from an external source to convert reactants into products. As a result, this adsorption reaction is nonspontaneous.

Acknowledgments

This work was supported by Scientific Research Projects Coordination Unit of Istanbul University. Project number 33692.

References

1. 1. K. Bon-Cheol, F. Danielle, S. Diane, K. Dong Wook, A. Heejoon, R. Jo Ann, B. Alexandre, K. Jayant, A. S. Lynne, Cross-Linked Multilayer Polymer-Clay Nanocomposites and Permeabilit, *J Macromol. Sci. Pure Appl Chem*., **41,** 1401 (2004).
2. D. Schmitt, A. Müller, Z. Csögör, F. H. Frimmel, C. Posten, The Adsorption Kinetics of Metal İons onto different Microalgae and Siliceous Earth, *Water Res*, **35**, 779 (2001).
3. A. M. Salleh Mohamad, M. Dalia Khalid, A. K. Wan Azlina Wan, I. Azni, Cationic and Anionic Dye Adsorption by Agricultural Solid Wastes: A Comprehensive Review, *Desalination*, **280**, 1 (2011).
4. J. Kuntal, D. Sudipta, Polygeneration using Agricultural Waste: Thermodynamic and Economic Feasibility study, *Renew. Energy*, **74**, 648 (2015).
5. L. Zhanguang, Z. Xuefei, C. Xiaohua, D. Chaomeng, Z. Juan, Z. Yalei, Biosorption of Lofibric Acid and Carbamazepine in Aqueous Solution by Agricultural Waste Ricestraw, *J. Environ. Sci.*, **25**, 2384 (2013).
6. M. Djebbar, F. Djafri, M. Bouchekara, A. Djafri, Adsorption of Phenol on Natural Clay, *Appli. Water Sci.*, **2**, 77 (2012).
7. T. Şişmanoğlu, Y. Kişmir, S. Karakuş, Single and Binary Adsorption of Reactive Dyes from Aqueous Solutions onto Clinoptilolite, *J. Hazard. Mat.*, **184**, 164 (2010).
8. Q. Sun, L. Yang, The Adsorption of Basic Dyes from Aqueous Solution on Modified Peat–Resin Particle, *Water Res*, **37**, 1535 (2003).
9. A. Andarge, R. Renuka, Development of Polymer Composite Beads for Dye Adsorption, *Int. J. Green Nanotechnol.*, **4**, 440 (2012).
10. C. Yin Kuo, C. H. Wu, J. Y. Wu, Adsorption of Direct Dyes from Aqueous Solutions by Carbon Nanotubes: Determination of Equilibrium, Kinetics and Thermodynamics Parameters, *J. Colloid Interface Sci.*, **327,** 308 (2008).
11. N. Sahiner, Colloidal Nanocomposite Hydrogel Particles, *Colloid & Polym. Sci.*, **285**, 413 (2007).
12. S. Y. Wong, Y. P. Tan, A. H. Abdullah and S. T. Ong, The Removal of Basic and Reactive Dyes Using Quartenised Sugar Cane Bagasse, *J. Phy. Sci.*, **20**, 59 (2009).
13. M. Juan, W. Won Sung, M. Jiho and Y. Yeoung-Sang, Removal of Basic Blue 3 from Aqueous Solution by *Corynebacterium glutamicum* Biomass: Biosorption and Precipitation Mechanisms, *Korean J. Chem. Eng*., **25**, 1060 (2008).
14. N. Ouazene and A. Lounis, Adsorption Characteristics of CI Basic Blue 3 from Aqueous Solution on Aleppo Pine-Tree Sawdust, *Color.Technol*., **128**, 21 (2011).
15. B. Karagozoglu, M. Tasdemir, E. Demirbas, M. Kobya, The Adsorption of Basic Dye (Astrazon Blue FGRL) from Aqueous Solutions onto Sepiolite, Fly Ash and Apricot Shell Activated Carbon: Kinetic and Equilibrium Studies, *J. Hazard. Mat.,* **147**, 297 (2007).
16. M. Wawrzkiewicz, Removal of C.I. Basic Blue 3 dye by Sorption onto Cation Exchange Resin,

Functionalized and Non-Functionalized Polymeric Sorbents from Aqueous Solutions and Wastewaters, *Chemical Engineering Journal*, **217**, 414 (2013).
17. V. Belesi, G. Romanos, N. Boukos, D. Lambropoulous, C. Trapalis, Removal of Reactive Red195 from Aqueous Solutions by Adsorption on the Surface of TiO_2 Nanoparticles, *J. Hazard. Mater*. **170**, 836 (2009).
18. Z. Chengjun, W. Qinglin, L. Tingzhou, I. I. Negulescu, Adsorption Kinetic and Equilibrium Studies for Methylene Blue Dye by Partially Hydrolyzed Polyacrylamide/ Cellulose Nanocrystalnanocomposite hydrogels, *Chem. Eng. J.*, **251**, 17 (2014).
19. C. Jun, L. Mingzhu, L. Hongliang and M. Liwei, Synthesis, Swelling and Drug Release Behavior of Poly (N,N-diethylacrylamide-co-N-hydroxymethyl acrylamide) hydrogel, *Mat.Sci.Eng.* C, **29**, 2116 (2009).
20. H. Hezaveh, I. I. Muhamad, Modification and swelling Kinetic Study of kappa-carrageenan-based hydro gel for Controlled Release Study, *J Taiwan Inst Chem Eng.*, **44**, 182 (2013).
21. Ç. Doğar, A. Gürses, M. Açıkyıldız and E. Özkan, Thermodynamics and Kinetic Studies of Biosorption of a basic Dye from Aqueous Solution Using Green Algae Ulothrix sp, *Coll. Surf. B: Biointerfaces*, **76**, 279 (2010).
22. A. Fakhri, Assessment of Ethidium Bromide and Ethidium Monoazide Bromide Removal from Aqueous Matrices by Adsorption on Cupric Oxide Nanoparticles, *Ecotox. Environ. Safe.*, **104**, 386 (2014).
23. Y. S. Ho, G. McKay, Pseudo-Second Order Model for Sorption Processes, *Process Biochemistry,* **34**, 451 (1999).
24. W. J. Weber, J. C. Morris, Kinetics of Adsorption on Carbon from Solution, *J. Sanit. Eng. Div. Am. Soc. Civ. Eng*., **89**, 31 (1963).
25. R. A. Khalid, Adsorption of Chlorinated Organic Compounds from Water with Cerium Oxide-Activated Carbon, *Arab. J. Chem,* (2015) , http://dx.doi.org/10.1016/j.arabjc.2015.04.013.
26. Z. Bekçi, Y. Seki, L. Cavas, Removal of Malachite Green by Using an İnvasive Marine Alga Caulerpa racemosa var, Cylindracea, *J. Hazard. Mat.*, **161**, 1454 (2009).
27. N. Sahiner, A. O. Yasar, Synthesis and Modification of p(VI) Microgels for in Situ Metal Nanoparticle Preparation and their Use as Catalyst for Hydrogen Generation from $NaBH_4$ Hydrolysis, *Fuel Process. Technol.,* **111**, 14 (2013).
28. A. C. Richards, I. J. Mccolm, J. B. Harness, Adsorption of Water by Anhydrous Nedocromil Sodium from 20 to 40^{o}C, *J. Pharm. Sci.*, **88**, 780 (1999).
29. W. Monika, Removal of C.I.: Basic Blue 3 Dye by Sorption onto Cation Exchange Resin Functionalized and Non-Functionalized Polymeric Sorbents from Aqueous Solutions and Wastewaters, *Chem. Eng. J.*, **217**, 414 (2013).
30. N. Ouazene, A. Lounis, Adsorption Characteristics of CI BasicBlue 3 from Aqueous Solution onto Aleppo Pine-Tree Sawdust, *Coloration Technology*, **128**, 21 (2012).
31. Shu-Wei Liew and Siew-Teng Ong, Removal of Basic Blue 3 Dye Using Pomelo Peel, *Asian J. Chem.*, **26**, 3808 (2014).
32. E. Demirbas, M. Kobya, A. E. S. Konukman, Error Analysis of Equilibrium Studies for the Almond Shell Activated Carbon Adsorption of Cr(VI) from Aqueous Solutions, *J. Hazard Mat***. 154**, 787 (2008).
33. Y. C. Wong a, Y. S. Szeto a, W. H. Cheung b, G. McKay, Adsorption of Acid Dyes on Chitosan Equilibrium Isotherm Analyses, *Process Biochem*. **39**, 693 (2004).
34. A. Kapoor, R. T. Yang, Correlation of Equilibrium Adsorption Data of Condensable Vapours On Porous Adsorbents*, Gas Sep. Purif*. **3**, 187 (1989).